Microscopy, 2022, **71(5)**, 297–301
DOI: https://doi.org/10.1093/jmicro/dfac030
Advance Access Publication Date: 17 June 2022
Article

MICROSCOPY

Real-time scanning electron microscopy of unfixed tissue in the solution using a deformable and electron-transmissive film

Seine A. Shintani*, Seiji Yamaguchi and Hiroaki Takadama

Department of Biomedical Sciences, College of Life and Health Sciences, Chubu University, 1200 Matsumoto-cho, Kasugai-shi, Aichi 487-8501, Japan
*To whom correspondence should be addressed. E-mail: shintani@isc.chubu.ac.jp

Abstract

It is difficult to use scanning electron microscopy to observe the structure and movement of biological tissue immersed in the solution. To enable such observations, we created a highly deformable and electron-transmissive polyimide film that can withstand the pressure difference between the high-vacuum electron column and the atmospheric-pressure sample chamber. With this film, we used scanning electron microscopy to measure the intrinsic fine structure and movement of the contractile fibers of excised mouse heart immersed in physiological solutions. Our measurements revealed that the excised heart is a dynamic tissue that undergoes relaxation oscillation based on a three-dimensional force balance.

Key words: scanning electron microscope, real-time electron microscopy, mechanical heart oscillation, electron microscopy of submerged samples, deformable and electron-transmissive film, sarcomeric oscillations

Introduction

The development of protein-labeling technologies, including the expression of fusion proteins with a green fluorescent protein (GFP), has popularized live imaging of the localization and movement of proteins of interest using optical microscopy [1]. We have also developed an optical microscopy method to measure the movement of an individual sarcomere with nanometer accuracy by expressing an α-actinin–GFP fusion protein in cardiomyocytes [2]. Using this live imaging method, we discovered that myocardial sarcomeres undergo cyclic contraction and relaxation at core body temperature, known as hyperthermal sarcomeric oscillation [3,4]. This oscillation rate remains constant during chaotic changes in the phase and amplitude of adjacent sarcomeres in response to intracellular Ca^{2+} concentration [5]. Mathematical simulations suggest that this property plays an important role in rapid diastole [4–7], and live imaging is a powerful tool that enables us to scrutinize such predictions.

Despite its advantages, optical microscopy cannot identify dense structures <200 nm owing to the diffraction of light, and high-resolution measurements approaching this limit also have an extremely thin depth of focus. In contrast, electron microscopy uses electron beams instead of visible light, which enables a resolution as high as ∼0.5 nm and a depth of focus ∼60 times larger than that achievable using an optical microscope with the same magnification. However, probing a sample with an electron beam must be done in a vacuum. As a result, live imaging of biological samples, where immersion in the solution is essential, is difficult to perform using electron microscopy. The NanoSuit method was developed to enable live imaging of the structure and movement of biological samples, but this involves covering the sample with a low-volatility substance such as glycerin that does not contain water [8,9]. Therefore, this method cannot be used to observe the structure and movement of samples that require water immersion. To image such samples, a membrane covering that has excellent electron transmission and can withstand the pressure difference between the high-vacuum electron column and the atmospheric-pressure sample chamber has been devised [10–14]. Since this method allows the observation of a sample immersed in the solution, live imaging may be possible.

Thin films of polyimide and graphene are deformable, resistant to high differential pressures, and exhibit excellent electron transmission [10–14]. However, these previous films cannot protect samples from electron beam damage. Therefore, we created a protective polyimide film that can deform in response to changes in the shape of living tissue and protect samples from electron beam damage. Using this deformable and electron-transmissive (DET) film, we devised and validated a method to observe the structure and movement of an excised heart immersed in the solution and the dynamics of crystals in the solution.

Materials and methods

Preparation of the DET film

Silicon nitride, a practical material with electron beam transparency, has been used as a protective thin film for

Received 23 December 2021; Revised 8 June 2022; Editorial Decision 12 June 2022; Accepted 14 June 2022

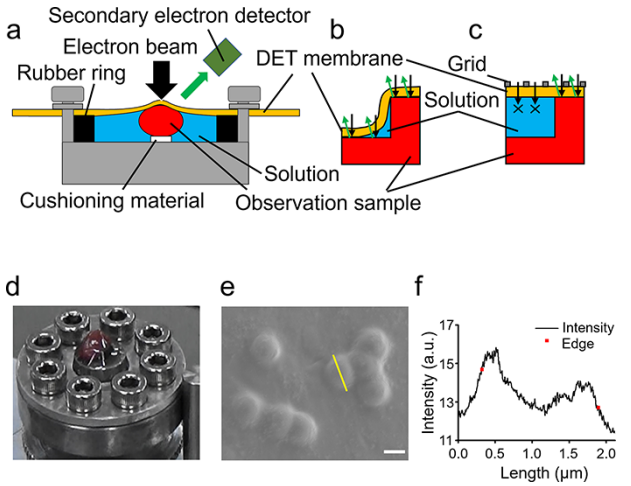

Fig. 1. Overview of the chamber used for mounting and covering the sample with a DET film for SEM analysis. (a) Schematic diagram of the sample chamber. (b, c) Schematic diagram of the positional relationship between the sample and the deformed (b) or non-deformed (c) DET film. (d) A photograph of the sample table during the dynamic analysis of the excised heart covered with polyimide-based DET film. (e) SEM image (1 keV, ×8 k) of 1 μm polystyrene beads covered with polyimide-based DET film. (f) Spatial dependence of the luminance along the yellow line in Fig. 1e. The distance between the red squares is the diameter of the hemispherical dome made by deforming the DET film over the surface of the beads.

electron microscopy [10,11] but has poor ductility and tears when deformed. We therefore used polyimide, which is also electron-transmissive but has excellent deformability and elasticity. Diphenyl-3,3′,4,4′-tetracarboxylic dianhydride was dissolved in *N*-methyl-2-pyrrolidone until the viscosity reached 5 Pa·s. The solution was then seeded on a borosilicate cover glass (C024321, Matsunami) and spread evenly using spin coating. The thickness h of the spin coat can be estimated using the formula $h \propto f^{-1}t^{-0.5}$, where f is the number of revolutions and t is the rotation time. We prepared a thin DET polyimide film by spin coating at 12 000 rpm for 30 s, then heating the cover glass at 400°C for 20 min in an electric furnace. A silicon rubber O-ring was placed on an aluminum sample table, then a sample was placed inside, immersed in the solution, and covered with the DET film. By pressing an annular stainless steel plate onto the DET membrane, a closed sample chamber was created (Fig. 1a). The thickness and shape of the DET film was adjusted by changing the height of a spacer placed under the sample and by varying the force applied by the stainless steel plate.

Sample preparation

This study followed an experiment plan approved by the Animal Experiment Committee of Chubu University. Hearts were excised from 3-week-old, isoflurane-anesthetized female ddY mice (Japan SLC, Inc.) and immersed in Dulbecco's Modified Eagle Medium (DMEM)/F-12, 15-m M 4-(2-hydroxyethyl)-1-piperazineethanesulfonic acid (HEPES) medium (Gibco, 11330032) supplemented with 10% v/v fetal bovine serum and 100 U mL^{-1} penicillin and streptomycin. To measure the shape and movement of a cross-sectional surface, the excised heart was cut at the interface between the ventricle and the atrium, a cushioning melamine sponge was used as a spacer, and the ventricular side was used for measurement. To measure the movement of the intact heart, a tall stainless steel cylinder was used as a spacer, with the height chosen to ensure that the movement of the heart would not be hindered by excessive DET film pressure. Solution sample experiments used the same medium in which the excised heart was immersed. To measure the deformation of the DET film, polystyrene beads with a diameter of 1 μm (Fluoresbrite YG Microspheres, Polysciences) were immersed in the solution and pressed against the DET film using a melamine sponge as a spacer.

Electron microscopy

Field-emission scanning electron microscopy (SEM) was performed using an S-4300 instrument (Hitachi High-Tech) together with the modified sample chamber, as shown in Fig. 1a.

Data analysis

Moving images could not be captured using the application interface of the SEM. Therefore, the video signal displayed on the monitor was recorded using a video capture system (400-MED1026, Sanwa Supply Inc.), and the observation area was cropped and analyzed using ImageJ software (National Institutes of Health) [15]. Origin(Pro), Version 9J (OriginLab Corporation) was used for data analysis and graph creation after digitization.

Statistical analysis

All statistical tests were performed using R software (www.r-project.org). The normality and homoscedasticity of the amplitudes and times of oscillation were tested using Kolmogorov–Smirnov and Bartlett tests. Multiple comparisons of data that satisfied both normality and homoscedasticity assumptions were performed using Dunnett's test; otherwise, Steel's multiple comparison test was used. The significance level for all analyses was 5%. The error bars in all figures indicate standard deviations.

Results

A schematic diagram (Fig. 1a–c) of the sample chamber, a photograph of the sample chamber during the analysis of the structure and movement of the excised heart (Fig. 1d) and an SEM image of a sample of 1-μM polystyrene beads (Fig. 1e and f) are shown. The deformability of the electron-transmissive film was utilized to observe the structure and movement of various sample shapes (Fig. 1b and c). The thickness of the DET film was derived from the SEM images by measuring the diameter of the hemispherical dome of 1-μm polystyrene beads covered with the DET film (Fig. 1e) and found to be 285.4 ± 40.2 nm (Fig. 1f, $n = 5$). The edge points for measuring the diameter corresponded to the inflection points obtained by fitting sigmoid functions.

The structure and movement of the cross-sectioned heart depended on the force with which the DET film was applied (Fig. 2). When it was strongly pressed against the heart, the movement of a fine uneven shape corresponding to the cross-sectional size and filamentous structure of a sarcomere could be observed (Fig. 2a–c, Supplementary Video 1). By reducing the pressure of the DET film slightly, it was possible to clearly observe the sarcomere cross-sectional shape and the overall movement of the heart (Fig. 2d–f, Supplementary Video 2).

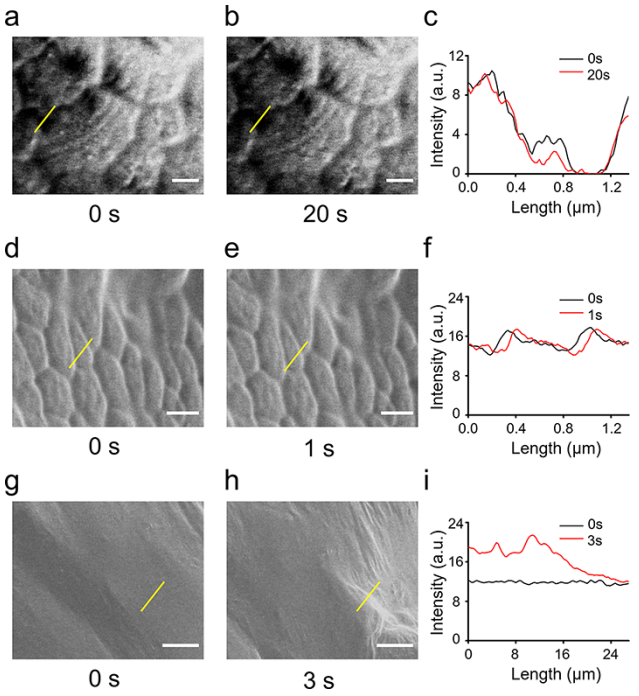

Fig. 2. SEM analysis of the structure and movement of a cross-section of the excised heart covered with polyimide-based DET film. (a–c) SEM images (3 keV, ×10 k) obtained with the film strongly pressed against the heart. (a, b) Images acquired 20 s apart (scale bar: 1 μm). Motion can be inferred from the black and red traces in (c), which show the intensity profiles along the yellow lines in (a) and (b), respectively. (d–f) SEM images (3 keV, ×12 k) obtained with the film pressed against the heart reasonably strongly. (d, e) Images acquired 1 s apart (scale bar: 1 μm). Motion can be inferred from the black and red traces in (f), which show the intensity profiles along the yellow lines in (d) and (e), respectively. (g–i) SEM images (1 keV, ×0.7 k) obtained with the film loosely pressed against the heart. (g, h) Images acquired 3 s apart (scale bar: 20 μm). Motion can be inferred from the black and red traces in (i), which show the intensity profiles along the yellow lines in (g) and (h), respectively.

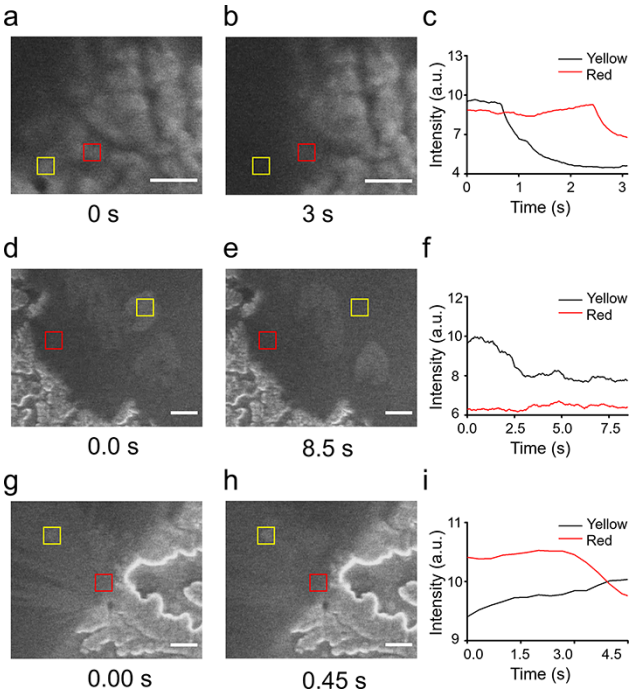

Fig. 3. SEM analysis of the structure and movement of precipitated crystals suspended in the solution beneath the DET film. (a–c) SEM images (5 keV, ×18 k) of crystals that precipitated directly under the DET film, applied an upward force on it and then sank into the liquid. (a, b) Images acquired 3 s apart (scale bar: 1 μm). The dynamics can be inferred from the black and red traces in (c), which show the time-dependent intensities within the yellow and red boxes, respectively. (d–f) SEM images (5 keV, ×2.5 k) of crystals moving around in the liquid directly under the DET film. (d, e) Images acquired 8.5 s apart (scale bar: 2 μm). The dynamics can be inferred from the black and red traces in (f), which show the time-dependent intensities within the yellow and red boxes, respectively. (g–i) SEM images (5 keV, ×6 k) of the dynamics of the boundary between crystals in contact with the DET film and those that are not. (d, e) Images acquired 0.45 s apart (scale bar: 2 μm). The dynamics can be inferred from the black and red traces in (i), which show the time-dependent intensities within the yellow and red boxes, respectively.

Further reduction of the DET film pressure made it possible to observe the dynamic movement of the heart (Fig. 2g–i, Supplementary Video 3). Therefore, by adjusting the pressure applied by the DET film, it was possible to selectively emphasize either fine structural detail or unrestricted, dynamic movements.

Analysis of the structure and movement of precipitated crystals suspended in the solution is shown in Fig. 3. By observing the surface of the DET film, we were able to monitor the dynamics of the following: crystals that precipitated directly under the DET film, applied an upward force on it, then sank into the liquid (Fig. 3a–c, Supplementary Video 4); crystals moving in the liquid beneath the film (Fig. 3d–f, Supplementary Video 5); the boundary between crystals that were in contact with the DET film and those that were not (Fig. 3g–i, Supplementary Video 6). Within the yellow frames in Fig. 3g–i, it was possible to distinguish crystals that pushed against the film from those that did not, and within the red frames, we could observe how the edges of crystals in contact with the DET film cracked and separated.

By pressing the sample against the DET film (Fig. 1a), air was excluded from entering between them (Fig. 2 and 3). Using an inverted SEM, the range of DET film mounting conditions under which air does not interfere with observation will be expanded.

Motion analysis of the excised heart is shown in Fig. 4. Slow and fast oscillations of the heart tissue were identified, together with very low-amplitude motions (nano-oscillations) (Fig. 4a and b). The large oscillations were analyzed by dividing them into slow and fast components, yielding periods of 12.55 ± 1.98 and 1.34 ± 0.24 s (Fig. 4c) and speeds of 0.0387 ± 0.0023 and $0.4864 \pm 0.0659\,\mu m\,s^{-1}$ (Fig. 4d), respectively, and a common amplitude of $0.579 \pm 0.099\,\mu m$ (Fig. 4f). The angle between the directions of the slow and fast motion vectors was ~180°, and the large periodic motion was confirmed to be continuous and reciprocating (Fig. 4e).

The nano-oscillations had a period of 0.56 ± 0.11 s (Fig. 4c), a velocity of $0.0705 \pm 0.007\,\mu m\,s^{-1}$ (Fig. 4d) and an amplitude of $0.0339 \pm 0.0057\,\mu m$ (Fig. 4f). On average, the direction of the nano-oscillations was orthogonal to that of the large oscillations (Fig. 4e).

Discussion

Using a polyimide-based DET film to maintain sample integrity, we observed the structure and movement of

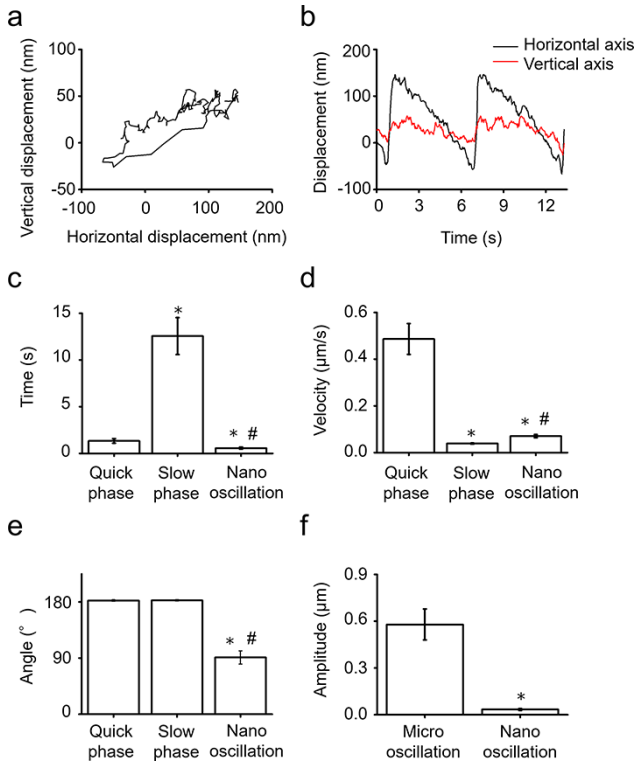

Fig. 4. SEM analysis of the movement of the excised heart tissue. (a) Representative trajectory for one cycle of periodic oscillation. (b) Time-dependence of the displacements shown in (a). Also shown are the (c) period, (d) velocity, (e) angle and (f) amplitude of the low-amplitude nano-oscillations and the slow and fast phases of large oscillations.

the excised heart immersed in the solution using SEM (Figs. 2 and 4). Previous studies used electron-transmissive silicon nitride film to cover samples obtained by antibody staining [10,11]. However, such a method does not permit measurements of the intact excised heart immersed in the solution. Since sample movement cannot be observed when the distance from the film is too large (Fig. 1c), the use of a film that is not only electron-transmissive but also deformable made it possible to observe a sample with a three-dimensional shape and movement (Fig. 1b). Using such a DET film therefore expands the size, shape, and range of movements of immersed samples that can be observed. Although the NanoSuit method can be used to study three-dimensional biological samples, they are covered with a non-volatile substance such as glycerin, making this method unsuitable for observing the structure and movement of biological samples requiring immersion in physiological solutions [8].

Analysis of the cross-sectioned heart showed that it was possible to adjust the pressure of the DET film against the sample surface to emphasize either structural or dynamic details (Fig. 2). The periodic motion was observed only when the DET film was pressed against a moving organ, such as the heart. Under the same conditions, there was no visible motion of inanimate organs (e.g. liver) or objects (e.g. melamine sponge). Based on these observations, we concluded that the movement of the sectioned heart was attributable to its intrinsic motion. Although movement could be limited by using a relatively high DET film pressure to enable structural observations, the deformability and elasticity of the film enabled dynamic observations by expanding and contracting in response to the movement of the sample.

In addition to the heart, the DET film was also used to monitor the structure and movement of crystals suspended in the solution (Fig. 3). This result showed that the DET film cannot only be used to study the structure and motion of biological samples but also chemical solutions and samples. We were able to analyze the dynamics of crystals that precipitated directly under the DET film, pushed against it and then sank into the liquid, which confirmed the dynamic deformability of the polyimide film (Fig. 3a–c). We also analyzed the motions of crystals beneath the DET film (Fig. 3d–f), which verified that the polyimide film has excellent electron transmission. It was also possible to observe the force of crystals against the DET film, which confirmed that the polyimide film is both electron-transmissive and deformable (Fig. 3g–i).

Using the DET film to obtain the time-dependent SEM images of the intact excised heart, we identified relaxation oscillations with an amplitude of ∼580 nm, accompanied by nano-oscillations with an amplitude of ∼34 nm (Fig. 4). As we previously reported, myocardial sarcomeres undergo cyclic contraction and relaxation [2–4]. This oscillation results from a combination of slow contraction of the sarcomere and rapid relaxation due to tension from the contraction of surrounding sarcomeres [2–5,16]. The amplitudes and velocities of the relaxation oscillations in Fig. 4 are within the ranges of those exhibited by sarcomeres [2–5,16] and thus believed to be genuine sarcomeric oscillations. Therefore, the observation that nano-oscillations were largely orthogonal to the orientation of the relaxation oscillations can be understood as a sarcomeric oscillation in another direction to maintain the balance of force. In that case, the direction normal to the DET film was such that the force balance is not disturbed. Since pumping of the heart involves coordinated motion of sarcomeres, it is possible that the force balance and resulting sarcomere oscillations will be multidirectional [6].

SEM analysis of the movement of the excised heart using a polyimide-based DET film showed that the organ is a dynamic tissue that undergoes relaxation oscillation based on the three-dimensional force balance. We believe that live imaging, which simultaneously measures structure and motion, is important for the analysis of such dynamic tissues. In addition to larger-scale motions, oscillations with an amplitude of 34 nm were identified, indicating that SEM combined with a DET film provides a unique method to sensitively capture nanoscale structures and motions.

Funding

Grants-in-Aid for Scientific Research from Japan (JP17K15102 and JP20K15762 to S.A.S.); Strategic Information and Communications R&D Promotion Programme of the Ministry of Internal Affairs and Communications of Japan; New Energy and Industrial Technology Development Organization (JPNP20004 to S.A.S.); Chubu University Production Technology Development Center research fund (Project (6) to S.A.S.); Chubu University special research fund (21M01CP to S.A.S.).

Acknowledgements

We would like to thank the laboratory students Yokoyama Yuichi and Imura Chisaki for supporting the experiment.

We would also like to thank the analysis center, work design room and laboratory animal education and research center of Chubu University for technical support. We thank Edanz (https://jp.edanz.com/ac) for editing a draft of this manuscript.

Supplementary data

Supplementary data are available at *Microscopy* online.

Author contributions

S.A.S., S.Y. and H.T. designed the research. S.A.S. designed the project, performed the experiments, analyzed the experimental data and wrote the paper. All authors have approved the final draft of the manuscript, and their contributions qualify them as authors.

Conflict on interest

The authors declare no conflicts of interest associated with this manuscript.

References

1. Matz M V, Fradkov A F, Labas Y A, Savitsky A P, Zaraisky A G, Markelov M L, and Lukyanov S A (1999) Fluorescent proteins from nonbioluminescent Anthozoa species. *Nat. Biotechnol.* 17: 969–973.
2. Shintani S A, Oyama K, Kobirumaki-Shimozawa F, Ohki T, Ishiwata S, and Fukuda N (2014) Sarcomere length nanometry in rat neonatal cardiomyocytes expressed with α-actinin-AcGFP in Z discs. *J. Gen. Physiol.* 143: 513–524.
3. Shintani S A, Oyama K, Fukuda N, and Ishiwata S (2015) High-frequency sarcomeric auto-oscillations induced by heating in living neonatal cardiomyocytes of the rat. *Biochem. Biophys. Res. Commun.* 457: 165–170.
4. Shintani S A, Washio T, and Higuchi H (2020) Mechanism of contraction rhythm homeostasis for hyperthermal sarcomeric oscillations of neonatal cardiomyocytes. *Sci. Rep.* 10: 20468.
5. Shintani S A (2022) Hyperthermal sarcomeric oscillations generated in warmed cardiomyocytes control amplitudes with chaotic properties while keeping cycles constant. *Biochem. Biophys. Res. Commun.* 611: 8–13.
6. Yoneda K, Okada J, Watanabe M, Sugiura S, Hisada T, and Washio T (2021) A multiple step active stiffness integration scheme to couple a stochastic cross-bridge model and continuum mechanics for uses in both basic research and clinical applications of heart simulation. *Front. Physiol.* 12: 712816.
7. Shintani S A (2022) Does the hyperthermal sarcomeric oscillations manifested by body temperature support the periodic ventricular dilation with each heartbeat? *Front. Physiol.* 13: 846206.
8. Takaku Y, Suzuki H, Kawasaki H, Ohta I, Ishii D, Hirakawa S, Tsutsui T, Matsumoto S, Takehara S, Nakane C, Sakaida K, Suzuki C, Muranaka Y, Kikuchi H, Konno H, Shimomura M, and Hariyama T (2017) A modified 'NanoSuit®' preserves wet samples in high vacuum: direct observations on cells and tissues in field-emission scanning electron microscopy. *Royal Soc. Open Sci.* 4: 160887.
9. Suzuki C, Takaku Y, Suzuki H, Ishii D, Shimozawa T, Nomura S, Shimomura M, and Hariyama T (2021) Hydrophobic-hydrophilic crown-like structure enables aquatic insects to reside effectively beneath the water surface. *Commun. Biol.* 4: 708.
10. Thiberge S, Nechushtan A, Sprinzak D, Gileadi O, Behar V, Zik O, Chowers Y, Michaeli S, Schlessinger J, and Moses E (2004) Scanning electron microscopy of cells and tissues under fully hydrated conditions. *Proc. Natl. Acad. Sci. U. S. A.* 101: 3346–3351.
11. Kristt D and Nyska A (2007) The wet tissue SEM — a new technology with applications in drug development and safety. *J. Toxicol Pathol.* 20: 1–11.
12. Stoll J D and Kolmakov A (2012) Electron transparent graphene windows for environmental scanning electron microscopy in liquids and dense gases. *Nanotechnology* 23: 505704.
13. Weatherup R S, Ern B, Hao Y, Bluhm H, and Salmeron M B (2016) Graphene membranes for atmospheric pressure photoelectron spectroscopy. *J. Phys. Chem. Lett.* 7: 1622–1627.
14. Arble C, Guo H, Matruglio A, Gianoncelli A, Vaccari L, Birarda G, and Kolmakov A (2021) Addressable graphene encapsulation of wet specimens on a chip for optical, electron, infrared and X-ray based spectromicroscopy studies. *Lab Chip* (The Royal Society of Chemistry) 21: 4618–4628.
15. Schindelin J, Arganda-Carreras I, Frise E, Kaynig V, Longair M, Pietzsch T *et al.* (2012) Fiji: an open-source platform for biological-image analysis. *Nat. Methods* 9: 676–682.
16. Shintani S A (2021) Effects of high-pressure treatment on the structure and function of myofibrils. *Biophys. Physicobiol.* 18: 85–95.